What Is the Role of the Helical Domain of Gs_α in the GTPase Reaction?†

Tamar Shnerb, Naama Lin, and Avital Shurki*,‡

Department of Medicinal Chemistry and Natural Products, The Lise Meitner-Minerva Center for Computational Quantum Chemistry, School of Pharmacy, The Hebrew University of Jerusalem, Jerusalem 91120, Israel

Received March 27, 2007; Revised Manuscript Received June 24, 2007

ABSTRACT: Structural analysis of Gs_α shows that it is composed of two domains: the ras-like domain (RD) that is conserved in all members of the GTPase superfamily and is homologous to the monomeric G-proteins (e.g., $p21^{ras}$) and an α-helical domain (HD) that is unique to heterotrimeric G-proteins. Little is known about the function of the HD. Recent experiments by Bourne and co-workers, who expressed both the RD and the HD of Gs_α separately and found that GTP hydrolysis is very slow if only recombinant RD is present but is accelerated when the HD is added, suggest that the HD serves as an intrinsic GTPase-activating protein (GAP). In this work, the GTP hydrolysis in Gs_α was studied. The results obtained by calculating catalytic effects with and without the HD provide evidence for the role of the HD as a GAP. It is demonstrated that a major part of the catalysis is obtained because of an allosteric influence of the HD on the RD. Structural as well as energetic considerations suggest that the HD confines the RD to a more compact conformation, pushing the phosphate into an orientation where it is further stabilized, thus lowering the overall reaction barrier. The resemblance between the behavior of rasGAP and the HD suggests that the conclusion may be a general conclusion, applicable for all of the G-protein members.

G-proteins transmit signals from cell surface receptors to effector proteins that modulate a wide variety of cellular processes. All G-proteins form a relatively stable complex with their substrate, GTP[1], and with the product of hydrolysis, GDP (*1*−*6*). The binding and hydrolysis of GTP trigger conformational changes that serve, in turn, to communicate with other proteins. The GTP and GDP bound forms define, respectively, the active and inactive states of the protein as a regulatory machine. There are two types of G-proteins: monomeric and heteromeric. Heterotrimeric G-proteins are composed of α and $\beta\gamma$ subunits, which are complexed together when bound to GDP. While binding to GTP, the heteromeric G-proteins undergo some conformational changes that result in the dissociation of the α subunit bound to the GTP (G_α-GTP) from the $G_{\beta\gamma}$ subunits. Both the G_α-GTP subunit and the $G_{\beta\gamma}$ subunits regulate the activity of different downstream effectors such as adenylyl cyclase, phospholipase C, and ion channels (*7*−*9*). Deactivation of G-proteins is a result of the hydrolysis of GTP to GDP and reassociation of the G_α with the $G_{\beta\gamma}$ subunits.

Structural analysis of Gs_α as well as other types of G_α subunits identified two distinct domains: the Ras-like domain (RD) also called the GTPase domain (*10*−*17*), and an α helical domain (HD) composed of six α helices that are inserted into the RD. The RD is homologous to the monomeric G-proteins (e.g., $p21^{ras}$) and is present in all members of the GTPase superfamily, whereas the HD is unique to the heterotrimeric G-proteins. Accordingly, while the different roles of the RD are well characterized, little is known about the HD. The different studies that addressed this question have put forward several proposals (*12*−*16*, *18*−*33*). Comparison of the amino acid sequences reveals large diversity in the HD (*3*, *14*), suggesting that the HD accounts for the specificity of the interactions of G_α with other proteins. Different studies have demonstrated the HD to serve as an effector recognition domain (*12*, *14*), or to participate in effector coupling and regulation (*18*−*21*). Other studies suggested that the HD is responsible for some of the interaction of G_α with receptors (*22*), with regulators of G-protein signaling (RGS) (*23*), or with the $G_{\beta\gamma}$ subunits (*24*). Structurally, the HD, together with the RD, create a cleft where the nucleotide is bound (*13*). Thus, several studies have examined the contribution of the HD in nucleotide binding and release (*25*−*28*). Finally, the intrinsic rate of GTP hydrolysis is about ∼1000-fold faster in G_α of heteromeric G-proteins compared to monomeric G-proteins (being about 1−5 min^{-1}) (*1*). However, when complexed with GTPase-activating proteins (GAPs), the monomeric G-proteins can hydrolyze GTP at rates of about 100-fold faster than that of G_α (*29*−*31*). Additionally, structural comparison between different G_α proteins and the complex of $p21^{ras}$ (ras hereafter) with rasGAP demonstrates that the location of the HD corresponds to the location of the GAP in the ras-rasGAP complex (i.e, (*14*−*16*, *32*)). These two observations led researchers to suggest that the HD serves as an intrinsic GAP (*28*). Others suggested that the HD participates in the inactive−active conformational transitions of G_α (*33*).

† This work was partially supported by The Israel Science Foundation Grants (Nos. 1317/05 and 1320/05) and by the Alex Grass Center for Drug Design and Synthesis of Novel Therapeutics, the Stephanie Gross foundation, and the Dreikurs Research Fund.

* Corresponding author. Phone: +972-2-675-8696. Fax: +972-2-675-7076. E-mail: avital@md.huji.ac.il.

‡ Affiliated with the David R. Bloom Center for Pharmacy, The Hebrew University of Jerusalem.

[1] Abbreviations: GTP, guanosine triphosphate; GDP, guanosine diphosphate; HD, helical domain; RD, Ras like domain; GAP, GTPase activating protein; TS, transition state; EVB, empirical valence bond; FEP, free energy perturbation.

10.1021/bi700585w CCC: $37.00
Published on Web 08/30/2007

The focus of this work is the role of the HD as an intrinsic GAP. Bourne and co-workers expressed both the RD and the HD separately as recombinant proteins of Gs_α, where in the RD recombinant, a short linker (not present in RD) was inserted (*28*). They found that GTP hydrolysis was very slow in the presence of the RD recombinant alone. Nevertheless, the hydrolysis rate was accelerated when the HD recombinant was also added to the solution (*28*). Moreover, they showed that mutation of Arg^{201} in the HD recombinant decreased the hydrolysis rate. They concluded that the HD serves as an intrinsic GAP and suggested that GAPs in general stimulate GTPase activity by both contributing a catalytic residue (a conserved arginine, e.g., Arg^{201} in Gs_α and Arg^{789} in rasGAP) and stabilizing an active conformation of the RD (*28*). Different studies have shown the importance of the conserved arginine for catalysis (e.g., (*5*, *34*, *35*)) both in the monomeric and heteromeric G-proteins. In contrast, the importance of the conformational effect of GAPs in general and the HD in particular on GTP hydrolysis remains obscure.

Here, we first verify the role of the HD as an intrinsic GAP and then try to understand its origins. In a recent computational study of GTP hydrolysis both in ras and ras-rasGAP, we demonstrated that rasGAP acts allosterically on ras, facilitating hydrolysis (*36*). Because of the similarity between the systems (ras and G_α proteins), it seems just reasonable that the effect of the HD on RD will be allosteric as in the ras-rasGAP.

The GTP hydrolysis in Gs_α is studied. Our study first quantitatively reproduces the catalytic effect of Gs_α. In agreement with the experimental results (*28*), our work shows supporting evidence for the role of the HD as a GAP by calculating catalytic effects with and without the HD as well as with and without the HD's electrostatic interactions. The findings support the idea that the HD of Gs_α serves as an internal GAP. The results also demonstrate that a major part of the catalysis is obtained because of the allosteric influence of the HD on RD in Gs_α. The resemblance between the behavior of the rasGAP and the HD of Gs_α led us to believe that this conclusion is not unique to the Gs_α but applies generally to all of the proteins of this family.

METHODS

The hydrolysis reaction is modeled using the empirical valence bond (EVB) approach (*37*−*39*). This method describes the reacting fragments using several valence bond (VB) states that correspond to a particular reaction mechanism. The method allows these VB states to mix and change their relative contribution along the reaction coordinate. (For a more detailed description of the method, see, e.g., refs *37*−*39*.) The parameters for the potential energy surface utilized here for the hydrolysis reaction in solution were taken from our previous studies (*36*) and were only slightly refined (see Table 1S and Figure 1S in Supporting Information). Recent ab initio studies of the hydrolysis mechanism of phosphate monoesters in solution proposed an associative mechanism with a relatively late transition state (*40*). Following these studies, the reaction path was described by the three VB states (Φ_1−Φ_3) depicted in Scheme 1. These states, representing the reactant, pentacoordinated, and product states, respectively, were utilized to describe the reaction. The free energy perturbation (FEP) (*41*, *42*) combined with umbrella sampling (US) (*37*, *43*−*45*) techniques were used to drive the system between the three different VB states, while evaluating the free energy profile.

Scheme 1: Three VB States That were Used to Describe the Reaction[a]

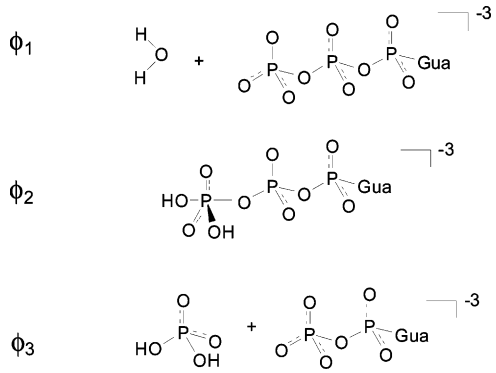

[a] Φ_1, Φ_2, and Φ_3 represent the reactant, pentacoordinated, and product states, respectively.

The simulations presented here were done using the ENZYMIX module of the program MOLARIS (*46*, *47*). Spherical systems of radius 18 Å were used with the boundaries restrained by the SCAAS model for the water molecules and by harmonic restraint to crystallographic positions for proteins (*48*). Long-range effects were treated by the local reaction field (LRF) long-range treatment (*49*). The starting coordinates used in the simulations of the Gs_α correspond to chain B in the 1AZT code taken from the Brookhaven Protein Data Bank (PDB) (*15*), where the sulfur atom in the GTPγS was replaced by an oxygen atom imposing an initial distance of 1.47 Å on that P_γ-O bond to obtain GTP. The simulations of the reaction profile considered Lys53, Arg201, and Asp223 to be explicitly ionized because of their expected importance to catalysis. Furthermore, a constraint of 3 kcal/mol was applied on the functional groups of both the Gln227 and Arg201 residues to their respective positions in the late transition state taken from a successful simulation. (See Supporting Information for more details.) The different computer simulations aimed at finding the role of the HD involved additional position constraints of different residues from the HD. Here again, the positions of the c_α in the residue of interest at the late transition state taken from one of the simulations of an unperturbed protein served as actual positions for the constraints. Finally, for all of the studies of the hydrolysis in the RD (in the absence of the HD), the α-carbons of Ile62, Leu63, Arg199, and Cys200 were constrained to their corresponding positions in Gs_α using a small harmonic constraint of 3 kcal/mol. The free energy profile for the overall reaction was evaluated after 200 ps of equilibration time, followed by 61 windows of 5 ps each for driving the system along the reaction coordinate using the FEP method. The errors for the convergence obtained by forward and backward integration of the same trajectories were found to range between 0.5 and 1.5 kcal/mol. Additionally, the simulations were carried out using various initial conditions (usually 4−6) in order to assess the accuracy of the results and to ensure proper average over the system's configurations (both in protein and in solution). The resulting error bar gave similar ranges. In two cases, which will be mentioned, the errors for the convergence obtained by forward and backward integration of the same

trajectories were found to range between 2 and 3 kcal/mol resulting in large overall energy differences between different initial conditions. In these cases, additional simulations were performed, and the final result is based on 8−10 different simulations.

The study of the contribution of separate residues to the overall stabilization of the nucleotide was carried out by using the linear response approximation (LRA) approach (*50*, *51*). This approach enables one to estimate the free energy difference between two potential surfaces U_1 and U_2 by the following equation:

$$\Delta G(U_1 \rightarrow U_2) = \frac{1}{2}(\langle U_2 - U_1\rangle_1 + \langle U_2 - U_1\rangle_2) \quad (1)$$

Here, $\langle\ \rangle_i$ designates an average over trajectories propagated on U_i. The use of LRA offers a unique ability to decompose free energies into additive contributions of individual residues, which cannot be accomplished by the FEP approach. In the present study, the contribution of different residues to the free energy difference between the pentacoordinated and the product states was estimated using this approach. Thus, the individual LRA contribution of the i^{th} group is given by the following equation:

$$\Delta G_i\,(U_{Int} \rightarrow U_P) = \frac{1}{2}(\langle U_P^i - U_{Int}^i\rangle_{Int} + \langle U_P^i - U_{Int}^i\rangle_P) \quad (2)$$

In order to obtain a reasonable estimate of the relative contributions of the different residues that would relate to the effect of their mutations, an effective dielectric constant was used, which scaled down the interactions with ionized residues by 20 and interactions of polar residues by 4 (see ref *52* for more details). Finally, the LRA calculations involved simulations of 20 ps on each state. All of the simulations were done at 300 K with a 1 fs time step.

RESULTS AND DISCUSSION

Reproducing the Catalytic Effect

Catalytic Effect of Gs_α. A prerequisite to any attempt at analyzing catalysis in biological systems is to have a reliable potential energy surface of these systems. In other words, in this study, prior to analyzing the role of the HD in catalysis, one has to establish the reliability of the EVB potential energy surfaces by reproducing the overall effect of Gs_α catalysis. The reaction involves a nucleophilic attack of the water molecule on the γ-phosphate and cleavage of the P_γ-O bond resulting with a hydrolyzed GDP and an inorganic phosphate. It is not clear, however, whether the uncatalyzed reaction follows an associative concerted mechanism with a late TS, as was recently proposed in the work of Klähn et al. (*40*) or whether a short-lived pentacoordinated intermediate exists, resulting in an associative stepwise mechanism as was earlier suggested (*36*). Therefore, we carried out two independent studies, examining the two possibilities. The overall picture obtained by the two mechanisms is very similar, and the presence of a stable intermediate in the solution reaction was found to have a negligible effect on the reaction profile in the protein (probably due to its overall low stability). Thus, we present here only the results obtained when the concerted mechanism is used to describe the uncatalyzed reaction, and those of the stepwise mechanism are given in Supporting Information (Figure 2S and Table 2S).

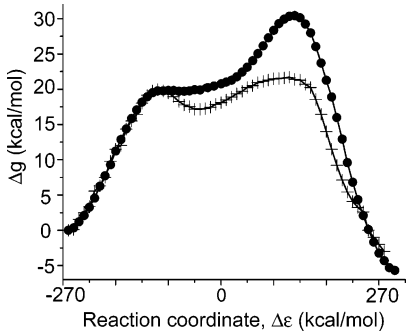

FIGURE 1: Free energy diagram for the GTP hydrolysis both in water (●), and Gs_α (+). EVB parameters were obtained by assuming a concerted free energy profile for the uncatalyzaed reaction profile. $\Delta\epsilon$ stands for the difference between the different VB states utilized to describe the reaction. Namely, the difference between Φ_1 and Φ_2 for the first half of the reaction and between Φ_2 and Φ_3 for the second half. For simplicity, a constant number was subtracted/added (for the first and second halves, respectively) to allow a uniform description of the reaction coordinate.

Table 1: Energetics of the GTPase Reaction in Water, Gs_α, Ras, and RasGAP[a]

	$\Delta g_1^{\ddagger}$	ΔG_1^0	$\Delta g_2^{\ddagger}$	$\Delta g_{cat}^{\ddagger}$ (calc)	$\Delta g_{cat}^{\ddagger}$ (exp)
water			27.9	27.9	27.9[b]
Gs_α	19.9	16.2	20.3	20.3	19.4[c]
ras[d]	15.2	11.9	23.2	23.2	22.2[e]
Ras-rasGAP[d]	16.1	9.0	13.5	16.1	≥15.9[e]

[a] $\Delta g_1^{\ddagger}$, ΔG_1^0, and $\Delta g_2^{\ddagger}$ correspond to free energies (in kcal/mol) of the first TS, pentacoordinated intermediate, and the second/late TS, respectively, relative to the reactants. The calculated results are an average over at least four different initial conditions. The activation energies were evaluated from the corresponding rate constants using transition state theory (*37*). [b] Taken from ref *58*. [c] k_{cat} is from refs *24* and *59*. [d] The calculated results are taken from ref *36*. [e] k_{cat} is taken from Schweins et al. (*60*). The inequality reflects the fact that the GTPase reaction might not be rate limiting in RasGAP.

The free energy profiles of both the catalyzed and uncatalyzed reactions resulting from the calculations are shown in Figure 1 and summarized in the first two entries in Table 1, along with the experimental results. The catalytic effect of the enzyme is evident. The results obtained for the hydrolysis in the protein suggest the formation of an intermediate, even when the solution reaction involves only a late transition state (*53*). These results are consistent with results obtained by Sucato et al. in their studies of nucleotidyl transfer, where similar mechanistic matters are encountered (*54*). In any case, since the calculated overall reaction barriers appear to be in relatively good agreement with available experimental data, reproducing the overall catalytic effect, and since we are not interested in the particular shape of the reaction profile but rather in its overall energetics, further studies on that system using this potential energy surface can, in principle, be meaningful (*55*).

The description of the uncatalyzed reaction as either concerted or as a stepwise mechanism was shown to have negligible influence on the overall picture of catalysis. Therefore, for simplicity of explanation, we will describe the reaction as a two-step hydrolysis regardless of energetics. Namely, the formation of a pentacoordinated state (either as an intermediate or with no particular energy definition),

will be considered the first step, and the cleavage of the P_γ-O bond resulting with the inorganic phosphate will be referred to as second step.

The results suggest that most of the catalytic effect takes place in the late TS of the reaction. It is rate limiting for the uncatalyzed reaction; thus, its stabilization leads to catalysis. For comparison with other systems, Table 1 lists the relative values of the energy profile of ras and the ras-rasGAP systems: entries 3 and 4 (*36*). Comparing the profiles for ras, ras-rasGAP, and Gs_α, it can be seen that ras stabilizes mainly the first stages of the reaction, Gs_α stabilizes mainly in the later stages of the reaction, whereas ras-rasGAP stabilization takes place along the whole reaction coordinate. Since the rate-limiting step in the solution reaction occurs in the late stages, the differences in the catalyzing abilities of these three systems is obvious. The origin of the differences between Ras, Gs_α, and RasGAP will be discussed in the following sections. Additionally, the fact that both Gs_α and ras-rasGAP but not ras stabilize mainly the late TS already supports the role of the HD in Gs_α, an intrinsic GAP, and is the subject of the next sections.

Evaluation of the Catalytic Effect of the Helical Domain. Reproducing the catalytic effect of Gs_α validated the potential energy surface of the system and thus enables us to go ahead and study the effect of the HD. The first step in this direction is the evaluation of the magnitude of the catalytic effect of the HD in Gs_α. Following the experiments of Bourne et al. (*28*), we decided to simulate GTP hydrolysis only in the RD. Since the effect of Arg201 is well known (*34*) and our goal is to find whether the HD has an additional role in catalysis, Arg201 was considered as part of the RD, although typically it is not present in other monomeric G-proteins. Thus, the coordinates of the sequence 63−199 were removed, leaving a model of the RD, which is designated by RD′(Gs_α), in the calculations. Moreover, since the HD is an insert sequence within the Gs_α, its deletion leaves two separate fragments that together form the RD′(Gs_α). In their experiments, Bourne et al. linked the two fragments by a small linker sequence (*28*). In our calculations, we wanted to avoid the addition of a new sequence since we would have to deal with the question of its exact conformation. Instead, the residues near the C- and N-termini of the HD in our RD′(Gs_α) model were restrained to their positions in Gs_α. That is, the α-carbons of the Ile62, Leu63, Arg199, and Cys200 in the RD′(Gs_α) were constrained to their corresponding positions in Gs_α using a small harmonic constraint of 3 kcal/mol. Finally, the hydrolysis reaction was simulated using the EVB approach. The results of these simulations are summarized in Table 2, along with the previous results for the native Gs_α (first two entries).

It is noted that these simulations were less stable and revealed larger sensitivity to different initial conditions. In any case, the activation free energy for GTP hydrolysis turned out to be ∼24 kcal/mol in the RD′(Gs_α) model instead of the ∼20 kcal/mol obtained in Gs_α. Namely, half of the catalytic effect of Gs_α is lost because of the absence of the HD, suggesting that its catalytic effect is about 4 to 5 kcal/mol. Since Arg201 was considered as part of RD′(Gs_α) in these calculations, it demonstrates that the HD has an additional role in catalysis other than contributing the catalytic Arg201. This result is in agreement with the results obtained for rasGAP in the ras-rasGAP complex (*36*).

Table 2: Energetics of the GTPase Reaction in Gs_α, and Its Different Analogues[a]

	entry	$\Delta g_1^\ddagger$	ΔG_1^0	$\Delta g_2^\ddagger$	$\Delta g_{cat}^\ddagger$
1	Gs_α	19.9	16.2	20.3	20.3 (19.4)[b]
2	RD′(Gs_α)	22.9	16.8	24.1	24.1
3	Gs_α-HD^{NP}	19.5	14.3	25.6	25.6
4	Gs_α-HD^{NP}(Asp173)[c]	18.9	13.2	20.7	20.7
5	Gs_α-HD^{NP}(Gln170)[c]	19.4	13.9	20.7	20.7
6	RD′(Gs_α)-Gln170[c]	21.3	15.5	24.1	24.1
7	RD′(Gs_α)-Asp173[c]	21.4	16.2	23.3	23.3

[a] $\Delta g_1^\ddagger$, ΔG_1^0, and $\Delta g_2^\ddagger$ correspond to free energies (in kcal/mol) of the first TS, pentacoordinated intermediate, and the second TS, respectively, relative to the reactants. The calculated results are an average over at least four different initial conditions. [b] The experimental value is within parentheses. [c] The residues that are mentioned explicitly are restrained at their c_α position.

Furthermore, the overall catalytic effect of RD′(Gs_α) of ∼4 to 5 kcal/mol is very similar to the ∼5 kcal/mol catalytic effect of ras, indicating that the RD′(Gs_α) indeed functions as a ras-like domain, whereas the HD indeed functions as an intrinsic GAP.

Next, we tested the exact role of the HD in catalysis. Two major catalytic roles could be attributed to the HD: a direct electrostatic effect where the HD residues directly stabilize the TS through electrostatic interactions or an allosteric effect in which the HD alters the shape of the RD to a more catalytic conformation, thus, accelerating its activity as found in the ras-rasGAP complex. The next section examines that question.

Exploring the Role of the Helical Domain

Gs_α Analogue with a Nonpolar Helical Domain. Electrostatic effects are computationally relatively easy to assess since they involve a fairly simple expression whose contribution to the calculations can be eliminated. Furthermore, electrostatic effects often play a major role in catalysis (*61*, *62*). Accordingly, our first attempt in the course of discovering the exact role of the HD involved abolishing its electrostatic contribution by mutating all of its residues into their nonpolar analogues. In other words, the partial charges of all of the HD residues (residues 63−199) were set to zero, thus, guaranteeing no electrostatic contribution. The resulting Gs_α analogue is referred to as Gs_α-HD^{NP}. The reaction profile resulting from the simulations of the GTP hydrolysis in Gs_α-HD^{NP} is given in the third entry in Table 2, along with the previous results for the native Gs_α (first entry). As can be seen, Gs_α-HD^{NP} resulted with loss of most of the catalytic effect of Gs_α. The overall activation barrier turned out to be ∼26 kcal/mol, which is ∼6 to 7 kcal/mol higher than the actual barrier for the native Gs_α. Moreover, this result is similar to, although slightly higher than, the activation barrier that was obtained when the HD was absent (the RD′(Gs_α) model). It is noted that here too the error bars were larger than the average ones.

On the basis of these results only, one might conclude that the role of the HD is entirely electrostatic. However, these results may be misleading because elimination of either the HD or its partial charges can also affect the overall structure of the RD, in which case the loss of catalysis would involve an allosteric effect as well. The instability of the results, suggested by the larger error bars and the dependence

of the results on the initial geometries, implies that the calculations involve changes in the overall structure of the RD and thus support the hypothesis of an allosteric effect. Therefore, additional experiments that would either confirm or rule out an allosteric influence should be carried out. Applying restraints on all of the residues of either the RD or the HD to their corresponding crystallographic structures cannot resolve the problem. G-proteins are flexible proteins, known to undergo some conformational changes when bound to GDP or GTP. Thus, restraining the whole structure of either the RD or the HD may impair hydrolysis.

A reasonable way to examine the allosteric effect can be achieved by keeping intact only important structural characteristics of Gs_α that are related to the interactions between the two domains (RD and the HD). In particular, Gs_α is known to have two pairs of salt bridges, Asp173-Lys293 and Gln170-Arg258, connecting the two domains (*33*, *63*). Salt bridges are usually known to be structurally important. In particular, Birnbaumer et al. have shown that mutating the Asp173 with Lys or Lys293 with Asp impaired the activity of Gs_α, whereas replacing both of them simultaneously (that is, applying both mutations together) restored the activity (*33*). The effect of salt bridges is known to be entirely related to their surrounding and the fact that the ion pair reversal restored the activity suggests that the local protein environment of the ion pair is probably not prepolarized (*64*). Thus, Birnbaumer's results emphasize the structural importance of this salt bridge, while challenging its electrostatic role. This experiment, therefore, gave us reason to believe that holding the salt bridge residues in their original position may keep the structure intact and thus enable us to learn about the electrostatic effect of the HD. Hence, in two parallel examinations, the c_α position of one HD residue that is involved in a salt bridge interaction with the RD (either Asp173 or Gln170) was restrained. Additionally, as done previously, the partial charges of all the HD residues were set to zero. The results are presented in entries 4 and 5 in Table 2. Looking at the results, it can be seen that most of the catalytic effect has been restored. The overall barrier is 20.7 kcal/mol, which is only slightly higher than the actual barrier. Moreover, the overall catalytic effect has been achieved, despite the fact that the HD did not contribute electrostatically. We can, therefore, conclude that the effect of this domain is not electrostatic. In other words, the HD residues do not have direct charge stabilization of elements in the reaction coordinate leading to catalysis. Furthermore, this result suggests that it is the position of the salt bridge residues rather than their respective charges that is important to catalysis, in agreement with the results of Birnbaumer et al. (*33*).

This result may lead to the conclusion that the role of the HD is merely to provide the salt bridges that will keep crucial parts of the active site in place. Thus, to gain further understanding, two additional simulations were carried out. The first examined whether the salt bridge unaccompanied by the HD could restore catalysis. Thus, the simulation involved the removal of the HD residues apart from one of the salt bridge residues, Asp173 or Gln170, and some residues in its vicinity (five from each side). Once more, the c_α position of Asp173 or Gln170 was restrained to its corresponding position in Gs_α. The results of these tests are shown in entries 6 and 7 in Table 2. As can be seen, most

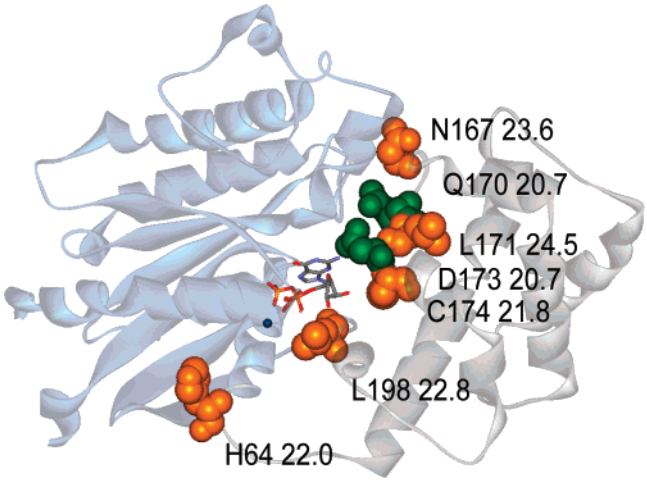

FIGURE 2: Illustration of the Gs_α, along with the residues whose c_α position was restrained, and the respective overall reaction barriers for the GTP hydrolysis obtained in simulations with these respective conditions. The RD′(Gs_α) is in blue, whereas the nonpolar HD is in gray. The different amino acids whose c_α position was restrained are highlighted in orange, along with their resulting reaction barriers, whereas the salt bridges and their respective results are in green.

of the catalytic effect of the HD disappeared, suggesting that the salt bridge by itself even if properly placed with respect to the RD cannot restore catalysis. In other words, the results imply that the presence of the HD is essential to establish the overall catalytic effect and that the salt bridge is responsible for only part of that catalytic role.

The second experiment examined whether the catalytic effect can be attributed to the positioning of any residue along the HD surface or whether it is unique to the salt bridges. Thus, several residues along the surface of the HD, which are in close proximity to the RD surface, were randomly selected, and the simulations involved placing restraints on their corresponding c_α positions. Each simulation involved the confinement of only *one* of the residues. Moreover, the partial charges of all of the HD residues were set to zero, resulting in a nonpolar HD. The various residues, along with the resulting overall barriers obtained from restraining their respective c_α positions, are presented in Figure 2.

As can be seen, different residues resulted in different overall barriers, ranging from ~21−22 for Cys174 and His64, where the catalytic effect of the HD is largely restored, gradually increasing with the various residues up to a barrier of ~24.5 for Leu171, where most of the HD catalytic effect is lost. It can be seen that not only the positions of the salt bridge residues but also the other residues along the HD interaction surface with the RD are important to catalysis, although to a lesser extent. For comparison, the results for the same simulation with the salt bridges are also presented in the Figure (highlighted in green). Careful examination of the results reveals that close proximity of the residue to the catalytic site is essential for a substantial effect of its position on the overall catalysis. Leu171 is positioned away from the RD; thus, its position has virtually no contribution to catalysis, whereas both the salt bridges and to a lesser extent other residues, such as Cys174 or His64, are positioned toward the RD and, thus, contribute to catalysis. Since none of the HD residues is charged, we concluded that the contribution is allosteric. It appears that the role of electro-

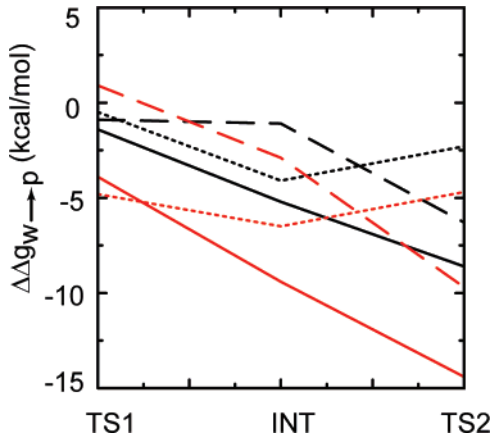

FIGURE 3: Stabilization energy of the substrate due to the protein environment relative to water. Gs_α related systems are colored black, whereas ras-rasGAP systems are colored red. The effect of the overall system (Gs_α and ras-rasGAP complex) depicted in solid lines, is presented along with the effect of different parts of the systems. Ras-like domains (RD′(Gs_α) and ras) are depicted by dotted lines, whereas GAP-like domains (HD(Gs_α) and rasGAP) are depicted in dashed lines.

statics of the HD in the native protein is, therefore, to retain its proper positioning relative to the RD active site. This result is in agreement with earlier studies of the ras-rasGAP complex, where the effect of GAP was also found to be allosteric.

Helical Domain as an Internal GAP. In view of the fact that the HD was found to serve as an internal GAP of Gs_α, evaluation of the similarities and differences between Gs_α and the ras-rasGAP complex can be valuable. For the purpose of comparison, we define the stabilization energy of a substrate due to protein environment relative to water as follows:

$$\Delta\Delta g^{Y}_{w\rightarrow p}(X) = \Delta g^{w}(X) - \Delta g^{Y}(X) \qquad (3)$$

where X denotes the substrate configuration along the reaction path (e.g., reactants, TS, pentacoordinated configuration, etc.), and Y is the protein environment (e.g., Gs_α, RD′(Gs_α), HD(Gs_α) ras, etc.). The relative energies were chosen such that the stabilization energy of the reactants, $\Delta\Delta g^{Y}_{w\rightarrow p}(RS)$, will be zero. The calculated values are summarized in Table 3S and illustrated graphically in Figure 3. Stabilization energies are shown for the configurations of the two transition states and the pentacoordinated state as found in the protein. We note that for convenience, the stabilization energies were measured relative to energies taken from the stepwise profile in water, but a similar trend is expected when using the same configurations from the concerted profile. In the Figure, black represents the Gs_α system, whereas red represents the ras-rasGAP system. In addition, stabilization energies in Gs_α and the ras-rasGAP complex (plain lines) are shown along with their respective building block pair of components RD′(Gs_α), ras (dotted lines) and HD(Gs_α), rasGAP (dashed lines).

Note that the contributions to the stabilization energies of both HD(Gs_α) and rasGAP were estimated as the difference in the catalytic effect of the whole system (Gs_α, ras-rasGAP complex), and its respective ras-like domain (RD′(Gs_α), ras). These contributions illustrate that the presence of the GAP-like domain (i.e., HD(Gs_α), rasGAP) makes the catalytic machinery of RD′(Gs_α) and ras several orders of magnitudes more efficient.

Looking at the various graphs in Figure 3, few trends are immediately apparent. First, both ras and the RD′(Gs_α) exhibit similar behavior, having a relatively constant stabilizing effect on the different stages along the reaction pathway. Second, the action of GAP-like domains is markedly different with respect to the ras-like domain; both rasGAP and HD(Gs_α) stabilize configurations from the later stages of the reaction (the second TS−TS2) significantly more than configurations from earlier stages (the first TS−TS1 or the intermediate). In addition, their stabilization is gradually increasing along the reaction coordinate. Finally, comparison of the absolute values shows that the stabilizing effect of the ras-rasGAP system is much stronger compared to Gs_α. Moreover, this effect is true not only with regards to the overall system, but individual contributions from both ras and rasGAP are also higher than the corresponding stabilization from RD′(Gs_α) and HD(Gs_α).

Helical Domain as an Internal Allosteric GAP. Structural Aspect. Our calculations indicate that the main contribution of the HD to catalysis is allosteric. Yet, further analysis of the results is crucial for elucidating the origins of this effect. Since the role is suggested to be mostly allosteric, it seems only reasonable to start by comparing structures of the RD of Gs_α from different simulations and see if and how they are affected by the HD. Figure 4a displays a snapshot describing the TS of the second step in GTP hydrolysis of two different simulations: simulation in Gs_α as a whole, where the HD is catalytic (backbone in blue and explicit molecules in sticks), taken from one of the simulations for entry 1 in Table 2, and simulation in Gs_α-HD^{NP}, where the HD did not participate in catalysis (backbone in pink and explicit molecules in fine lines), taken from the simulations of entry 3 in Table 2. Thus, the former (blue) structure will be referred to as the catalytic structure and the latter (pink) as the less catalytic structure. The backbones of the p-loop and switches I and II of the RD of Gs_α are presented along with Thr204, Mg^{+2}, and the nucleotide.

Looking at the results, differences can be observed mainly in the structures of both the backbone of switch I and the nucleotide. In the less catalytic structure (seen in the Figure as fine lines), switch I seems to be drawn away from the nucleotide. This, in turn, leads to an overall increase in the distance of the conserved residue Thr204 from both the nucleotide and the Mg^{2+} ion. This distance increase causes the loss of most of the hydrogen bonds of Thr204 with the γ-phosphate as well as the loss of its location in the coordination sphere of the Mg^{2+}, thus probably lowering their stabilizing contribution. In fact, similar differences although larger in magnitude were observed in the Gt_α protein when the crystal structures of the GDP and GTP bound forms were compared (*16*).

Further inspection of Figure 4a reveals that the catalytic structure involves changes in several dihedral angles in the vicinity of the pentacoordinated phosphate of the nucleotide leading it into an orientation that is different from its initial orientation. These changes do not occur in the less catalytic structure, implying that they are triggered by the presence of the HD.

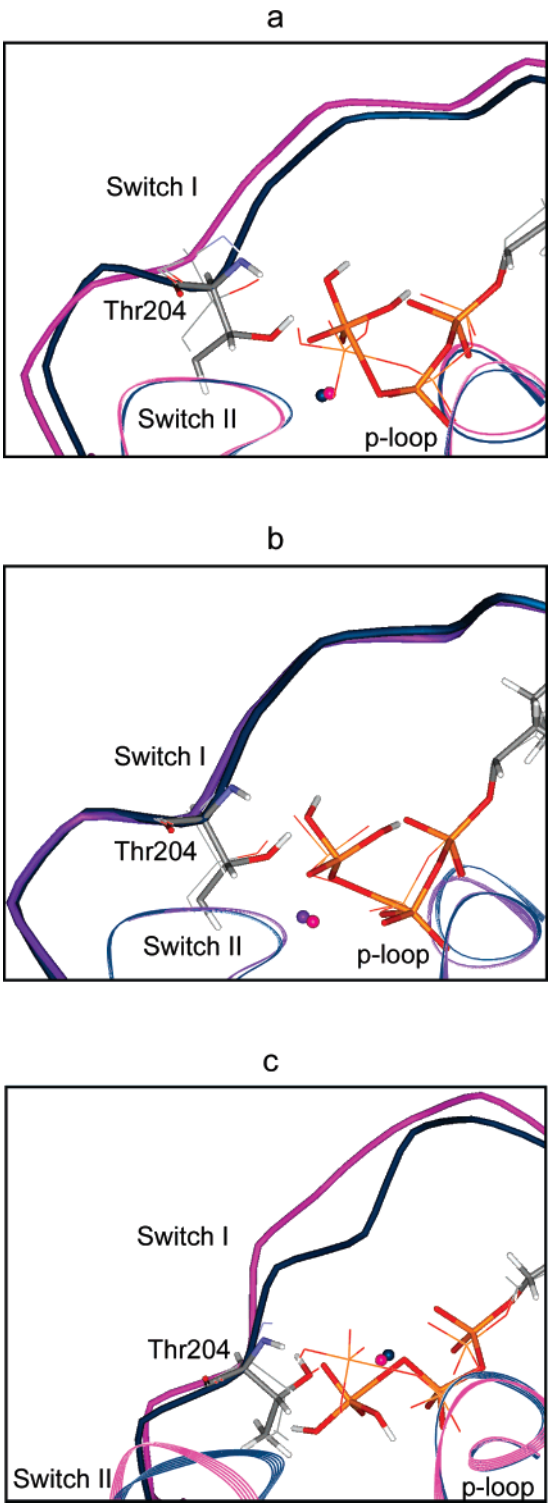

FIGURE 4: (a) Comparison of the active site structure of native Gs_α (blue backbone and stick format of atoms) to its structure when the HD does not contribute to catalysis, Gs_α-HD^{NP} (pink backbone and fine line format of atoms). (b) Comparison of the active site structure of native Gs_α (blue backbone and stick format of atoms) to its structure where the HD is nonpolar but contributes to catalysis because of the restraint of Asp173 to its proper position (not within the outskirts of the figure), Gs_α-HD^{NP}(Asp173) (purple backbone and fine line format of atoms). (c) Comparison of the active site structures of the ras-rasGAP complex (blue backbone and stick format of atoms) and ras (pink backbone and fine line format of atoms). The systems (ras-rasGAP and Gs_α) are adjusted to have the same orientation. The backbones of the p-loop, Switch I, and Switch II are presented along with the conserved threonine, Mg^{+2}, and the nucleotide in a geometry that corresponds to the second TS.

In order to verify whether these structural changes are significant, Figure 4b compares two catalytic structures: the structure of the second TS in the native protein (backbone in blue and explicit molecules in sticks, taken from simulations described by entry 1 in Table 2) and a nonpolar catalytic structure where the HD does not have any electrostatic contribution, but Asp173 is held in its proper position (backbone in purple and explicit molecules in fine lines, taken from simulations described by entry 4 in Table 2). Looking at the Figure, it can be seen that here indeed small differences are observed between the two structures. More details are available as Supporting Information.

Since our focus in this study is the HD as a GAP, it can be useful to compare the structural differences detected here because of the loss of HD to actual structural consequences due to complexation of a G-protein with GAP. The system chosen for this comparison is that of ras. For a sensible comparison, we performed simulations of GTP hydrolysis in both ras and ras-rasGAP and, as previously done (*36*), examined the structures of the second TS where the phosphate group is leaving. Figure 4c depicts the corresponding snapshots of ras (pink and fine lines) versus ras-rasGAP complex (blue and stick format). Only p-loop and switches I and II are presented along with the nucleotide in an orientation that is equivalent to that chosen for the Gs_α. Similar to the Gs_α, switch I seems to be drawn toward the nucleotide in the ras-rasGAP complex. It can also be seen that the original orientation of the pentacoordinated phosphate changes because of the presence of rasGAP. Looking at the Figure, as expected, the structural differences detected between the ras and the complex ras-rasGAP are slightly larger than those observed in the Gs_α system (Figure 4a), in agreement with the larger catalytic effect of GAP.

The resemblance in the structural differences suggests that both the HD and GAP operate in an analogous manner to enhance catalysis. Moreover, on the basis of this pictorial presentation, we suggest that the presence of either GAP or the HD confines the RD into a more compact conformation, which appears to be preferable for GTP hydrolysis since it probably pushes the phosphate into an orientation where is it further stabilized. We note here that while only one snapshot is presented we examined different snapshots in different simulations and observed the same trends, suggesting therefore that the observations are reliable. Nevertheless, these pictorial representations cannot establish a firm sense of understanding since structural changes cannot be converted into changes in energy in a straightforward manner, and a more quantitative approach is thus required.

Helical Domain as an Internal Allosteric GAP. Energetic Aspect. Similar to our earlier studies of the effect of rasGAP in the ras-rasGAP complex (*36*), we employed the LRA approach to analyze the electrostatic interactions between the nucleotide and individual residues of only the RD, with and without the effect of the HD. Figure 5 presents changes in the electrostatic interactions of the RD residues (residues 35−62 and 200−391) with the reacting fragments because of structural effects caused by the presence of the HD. As the late/second TS of the reaction is both rate-limiting step and the step where most of the energetic changes occur, the changes in the electrostatic contributions of both the pentacoordinated intermediate and product states are compared (Figure 5a and 5b, respectively). The changes were calculated

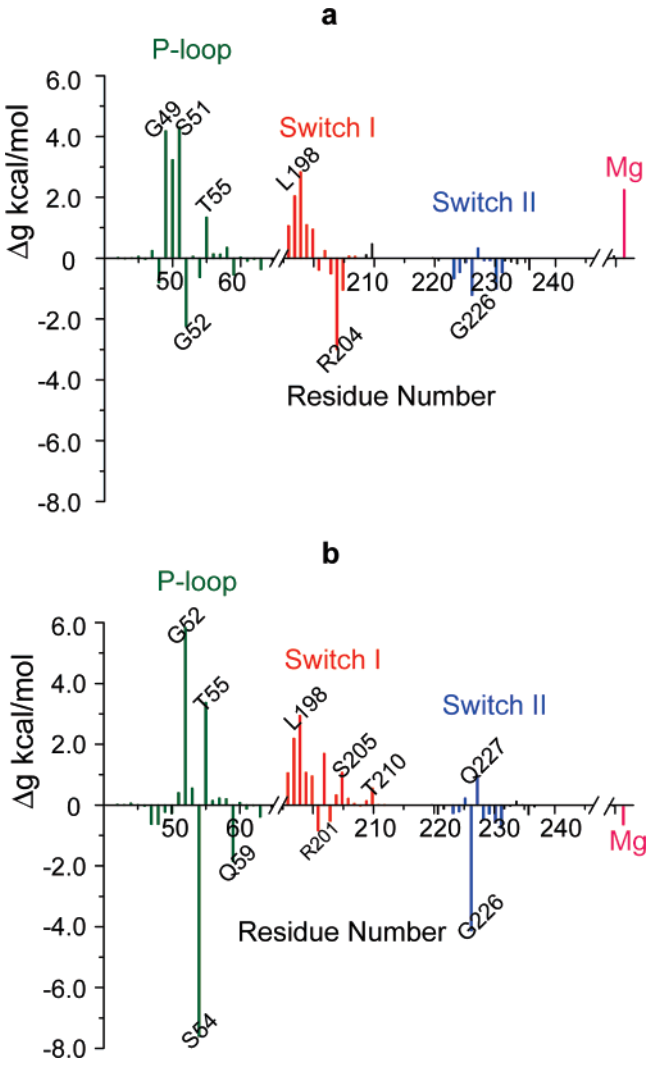

FIGURE 5: Changes in the electrostatic interactions of the RD residues with the reacting fragments (nucleotide) due to structural effects caused by the presence of the HD (RD → Gs_α). a and b present changes in the pentacoordinate intermediate and product states, respectively. Negative and positive values stand, respectively, for stabilization and destabilization due to the presence of the HD. Contributions of active site residues are colored green, red, and blue for p-loop, switch-I, and switch-II residues, respectively.

as the difference in the electrostatic contribution of the residues taken from simulations of Gs_α and Gs_α-HD^{NP}. Furthermore, since we are looking only at changes in the contribution of the RD residues, the HD residues (residues 63−199) were eliminated from the Figure. In addition, since the changes in the contribution of residues 249−391 is virtually zero, they were eliminated from the figure as well. Negative contributions correspond to a stabilizing effect of the HD on the RD residues, whereas positive contributions represent destabilization effects due to the presence of the HD.

As expected, most of the changes occur in the active site region, namely, the p-loop, switches I and II, and the Mg^{2+} ion (highlighted in different colors). The overall effect of the HD on the RD residues, obtained by summing up all the individual contributions, is destabilizing both in the intermediate and the product. In other words, the presence of the HD appears to weaken the stabilizing interactions of the RD residues with the reacting fragments. However, comparison of Figure 5a and b demonstrates (when summing up all the contributions) that this destabilization effect of the HD, which is relatively large in the pentacoordinated intermediate state, is largely reduced in the product state.

Scheme 2: Schematic Presentation of the Energy Profile of the Second Step of the Hydrolysis Reaction with (Blue) and without (Pink) the Effect of the HD

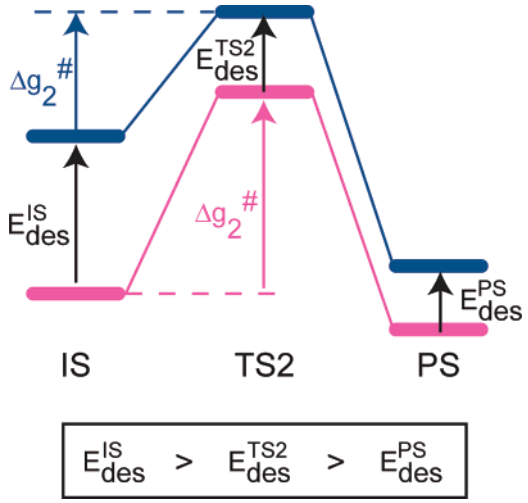

In order to better understand these results, they are summarized in Scheme 2. Here, the energy profiles of the second step of the reaction in the Gs_α with (blue lines) and without (pink lines) the effect of the HD are compared schematically. It is noted that the absolute location of the profiles along the energy scale has no significance, and we shall regard only the trends suggested by the relative energies within each profile. Following the results shown in Figure 5, the intermediate state destabilizes more than the product because of the presence of the HD. This reduced destabilization of the product state results with its overall stabilization relative to the intermediate state. The resulting effect of the HD at the TS is likely to be affected by both the intermediate and product states. Therefore, on the basis of the LFER approximation, the effect of the HD at the TS is predicted to be destabilizing, with a value that is lower than that of the intermediate and yet higher than that of the product. As seen in Scheme 2, this in turn leads to a lower overall barrier. This result suggests, therefore, that the HD confines the RD into a conformation, which favors the product state, thus reducing the reaction barrier. Finally, a comparable effect was found for the rasGAP in the ras-rasGAP complex, where it was suggested to allosterically affect the conformation of ras, turning it into a more catalytic conformation.

CONCLUDING REMARKS

In this work, we have studied the GTP hydrolysis reaction in Gs_α and examined the role of the helical domain. It was shown that most of the catalytic effect of the protein takes place in the second step of the reaction, where the phosphate group is leaving. Removal of the HD was found to cause loss of catalysis, indicating, in agreement with previous studies (*28*), that the HD is essential for the catalytic effect. In addition, elimination of the electrostatic contributions of the HD by converting it to its nonpolar analogue resulted in the restoration of catalysis when important structural features of the protein were kept intact. This indicates that the HD enhances the reaction rate by an allosteric rather than an

electrostatic effect. More specifically, on the basis of both structural and energetic evidence, it is shown that the HD both confines the RD and the phosphate into an orientation where the product is further stabilized, yielding a better catalytic conformation. Consequently, the reaction barrier is lowered, and the HD is found to allosterically improve catalysis mainly in the second step.

Our findings are consistent with the results of several experimental studies. In particular, Birnbaumer et al. proposed that the Asp173-Lys298 salt bridge between the HD and the RD in Gs_α is required for the proper positioning of the two domains with respect to each other (*33*). Supporting their conclusions, our simulations show that despite absence of any electrostatic contribution from the HD, virtually all of the catalytic effect is retained when the suitable position of the salt bridge is kept. Furthermore, in their study, they found that the proper positioning of the HD and the RD by the salt bridges is essential for G-protein activation by aluminum fluoride (TS analogue) but not by GTPγS (reactant state analogue). Our studies offer a simple explanation to this experimental observation. We showed that the HD affects mainly the second step of the reaction where most of the catalytic effect takes place. Therefore, interruption of the intramolecular domain interactions caused by mutations of one of the salt bridges, which is similar to turning off the charges of the HD, is unlikely to impede the first step of the reaction where the GTPγS binds. However, the same interruption, (i.e., loss of intramolecular domain interactions caused by mutation of one of the salt bridges) is expected to affect the second step of the reaction and thus results in the inability to achieve proper transition state configuration and, consequently, in the loss of ability to bind the transition state analogue AlF_4.

The G-protein superfamily is known to have a conserved glutamine residue in the active site, which is known to play an important role in hydrolysis. Mutations of this conserved glutamine in the two systems discussed (Gln227 in Gs_α or Glu61 in ras) have a similar effect on hydrolysis. Since glutamine 61 was shown to have an allosteric effect rather than a direct electrostatic effect on catalysis in the ras system, we believe that the effect of Gln227 on hydrolysis in Gs_α is also allosteric. This issue should be tested in future work.

There is an ongoing debate regarding the mechanism for GTP hydrolysis (dissociative/associative; for overview see, e.g., refs *40*, *65*, and *66*). Here, following our previous work and a more recent work of Klähn et al., we employed a more associative mechanism (*36*) and were able to reproduce catalysis in a very good agreement with observed reaction rates. An earlier work on the ras and rasGAP systems utilized both associative and dissociative mechanisms and showed that the role played by rasGAP in the ras-rasGAP complex is the same for both reaction mechanisms (*36*, *67*). Thus, since the role of the HD is similar to that of GAP we believe our results are also independent of the chosen reaction mechanism.

Finally, it is interesting to note that our conclusion about the allosteric action of HD is consistent with experimental studies done on other G-proteins. For example, HD is allosterically involved in activating retinal cyclic GMP phosphodiesterase by the transducin α subunit(Gtα) (*20*) and in stimulating adenylyl cyclase (*19*). We would therefore expect that HD could be involved as an allosteric modulator in many biological activities and that the HD influence may represent a common feature among all the members of the heterotrimeric G-protein family.

ACKNOWLEDGMENT

We thank Dr. Marek Strajbl for enlightening discussions.

SUPPORTING INFORMATION AVAILABLE

Parameters used for the reacting fragments in the EVB calculations (Table 1S and Figure 1S), along with some computational details, a stepwise reaction profile (Figure 2S, Table 2S), a table of stabilization energies that create Figure 3 (Table 3S) and quantitative evaluation of the structural differences observed in Figure 4 (Tables 4S and 5S). This material is available free of charge via the Internet at http://pubs.acs.org.

REFERENCES

1. Gilman, A. G. (1987) G-Proteins: transducers of receptor-generated signals, *Annu. Rev. Biochem. 56*, 615−649.
2. Bourne, H. R., Sanders, D. A., and McCormick, F. (1990) The GTPase superfamily: a conserved switch for diverse cell functions, *Nature 348*, 125−132.
3. Simon, M. I., Strathmann, M. P., and Gautam, N. (1991) Diversity of G proteins in signal transduction, *Science 252*, 802−808.
4. Kaziro, Y., Itoh, H., Kozasa, T., Nakafuku, M., and Satoh, T. (1991) Structure and function of signal-transducing GTP-binding proteins, *Annu. Rev. Biochem. 60*, 349−400.
5. Sprang, S. R. (1997) G Protein mechanisms: insights from structural analysis, *Annu. Rev. Biochem. 66*, 639−678.
6. Hamm, H. E. (1998) The many faces of G protein signaling, *J. Biol. Chem. 273*, 669−672.
7. Clapham, D. E., and Neer, E. J. (1993) New roles for G-protein beta-gamma-dimers in transmembrane signaling, *Nature 365*, 403−406.
8. Clapham, D. E., and Neer, E. J. (1997) G protein beta gamma subunits, *Annu. Rev. Pharmacol. Toxicol. 37*, 167−203.
9. Skiba, N. P., and Hamm, H. E. (1998) How Gs alpha activates adenylyl cyclase, *Nat. Struct, Biol*, *5*, 88−92.
10. DeVos, A. M., Tong, L., Milburn, M. V., Matias, P. M., Jancarik, J., Noguchi, S., Nishimura, S., Miura, K., Ohtsuka, E., and Kim, S. H. (1988) 3-Dimensional structure of an oncogene protein: catalytic domain of human c-H-Ras P21, *Science 239*, 888−893.
11. Pai, E. F., Kabsch, W., Krengel, U., Holmes, K. C., John, J., and Wittinghofer, A. (1989) Structure of the guanine-nucleotide-binding domain of the Ha-Ras oncogene product P21 in the triphosphate conformation, *Nature 341*, 209−214.
12. Masters, S. B., Stroud, R. M., and Bourne, H. R. (1986) Family of G-protein alpha-chains: amphipathic analysis and predicted structure of functional domains, *Protein Eng. 1*, 47−54.
13. Noel, J. P., Hamm, H. E., and Sigler, P. B. (1993) The 2.2 Å crystal structure of transducin-alpha complexed with GTP-gamma-S, *Nature 366*, 654−663.
14. Coleman, D. E., Berghuis, A. M., Lee, E., Linder, M. E., Gilman, A. G., and Sprang, S. R. (1994) Structures of active conformations of $G_{i\alpha1}$ and the mechanism of GTP hydrolysis, *Science 265*, 1405−1412.
15. Sunahara, R. K., Tesmer, J. J. G., Gilman, A. G., and Sprang, S. R. (1997) Crystal structure of the adenylyl cyclase activator G(S alpha), *Science 278*, 1943−1947.
16. Lambright, D. G., Noel, J. P., Hamm, H. E., and Sigler, P. B. (1994) Structural determinants for activation of the alpha-subunit of a heterotrimeric G protein, *Nature 369*, 621−628.
17. Lambright, D. G., Sondek, J., Bohm, A., Skiba, N. P., Hamm, H. E., and Sigler, P. B. (1996) The 2.0 Å crystal structure of a heterotrimeric G protein, *Nature 379*, 311−319.
18. Benjamin, D. R., Markby, D. W., Bourne, H. R., and Kuntz, I. D. (1995) Solution structure of the GTPase-activating domain of alpha(S), *J. Mol. Bio. 254*, 681−691.
19. Antonelli, M., Birnbaumer, L., Allende, J. E., and Olate, J. (1994) Human-xenopus chimeras of G(S)alpha reveal a new region important for its activation of adenylyl-cyclase, *FEBS Lett. 340*, 249−254.

20. Liu, W., Clark, W. A., Sharma, P., and Northup, J. K. (1998) Mechanism of allosteric regulation of the rod cGMP phosphodiesterase activity by the helical domain of transducin alpha subunit, *J. Biol. Chem. 273*, 34284−34292.
21. Liu, W., and Northup, J. K. (1998) The helical domain of a G protein alpha subunit is a regulator of its effector, *Proc. Natl. Acad. Sci. U.S.A. 95*, 12878−12883.
22. Krieger-Brauer, H. I., Medda, P. K., Hebling, U., and Kather, H. (1999) An antibody directed against residues 100−119 within the alpha-helical domain of G alpha(s) defines a novel contact site for beta-adrenergic receptors, *J. Biol. Chem. 274*, 28308−28313.
23. Skiba, N. P., Yang, C. S., Huang, T., Bae, H., and Hamm, H. E. (1999) The alpha-helical domain of G alpha(t) determines specific interaction with regulator of G protein signaling 9, *J. Biol. Chem. 274*, 8770−8778.
24. Graziano, M. P., and Gilman, A. G. (1989) Synthesis in *Eschesichia coli* of GTPase-deficiect mutants of $G_{s\alpha}$, *J. Biol. Chem. 264*, 15475−15482.
25. Warner, D. R., and Weinstein, L. S. (1999) A mutation in the heterotrimeric stimulatory guanine nucleotide binding protein alpha-subunit with impaired receptor-mediated activation because of elevated GTPase activity, *Proc. Natl. Acad. Sci. U.S.A. 96*, 4268−4272.
26. Grishina, G., and Berlot, C. H. (1998) Mutations at the domain interface of G(s alpha) impair receptor-mediated activation by altering receptor and guanine nucleotide binding, *J. Biol. Chem. 273*, 15053−15060.
27. Echeverria, V., Hinrichs, M. V., Torrejon, M., Ropero, S., Martinez, J., Toro, M. J., and Olate, J. (2000) Mutagenesis in the switch IV of the helical domain of the human Gs alpha reduces its GDP/GTP exchange rate, *J. Cell. Biochem. 76*, 368−375.
28. Markby, D. W., Onrust, R., and Bourne, H. R. (1993) Separate GTP-binding and GTPase-activating domains of a G-alpha-subunit, *Science 262*, 1895−1901.
29. Eccleston, J. F., Dix, D. B., and Thompson, R. C. (1985) The rate of cleavage of GTP on the binding of Phe-transfer RNA. Elongation factor Tu. Gtp to poly(U)-programmed ribosomes of *Escherichia-coli*, *J. Biol. Chem. 260*, 6237−6241.
30. Martin, G. A., Viskochil, D., Bollag, G., McCabe, P. C., Crosier, W. J., Haubruck, H., Conroy, L., Clark, R., Oconnell, P., Cawthon, R. M., Innis, M. A., and McCormick, F. (1990) The gap-related domain of the neurofibromatosis type-1 gene-product interacts with Ras P21, *Cell 63*, 843−849.
31. Gideon, P., John, J., Frech, M., Lautwein, A., Clark, R., Scheffler, J. E., and Wittinghofer, A. (1992) Mutational and kinetic analyses of the GTPase-activating protein (GAP)-p21 interaction: the C-terminal domain of GAP is not sufficient for full activity, *Mol. Cell. Biol. 12*, 2050−2056.
32. Scheffzek, K., Ahmadian, M. R., Kabsch, W., Wiesmuller, L., Lautwein, A., Schmitz, F., and Wittinghofer, A. (1997) The Ras-RasGAP complex: structural basis for GTPase activation and its loss in oncogenic Ras mutants, *Science 277*, 333−338.
33. Codina, J., and Birnbaumer, L. (1994) Requirement for intramolecular domain interaction in activation of G-protein alpha-subunit by aluminum fluoride and GDP but not by GTP-gamma-S, *J. Biol. Chem. 269*, 29339−29342.
34. Freissmuth, M., and Gilman, A. G. (1989) Mutations of Gs-alpha designed to alter the reactivity of the protein with bacterial toxins: substitutions at Arg187 result in loss of GTPase activity, *J. Biol. Chem. 264*, 21907−21914.
35. Ahmadian, M. R., Stege, P., Scheffzek, K., and Wittinghofer, A. (1997) Confirmation of the arginine-finger hypothesis for the GAP-stimulated GTP-hydrolysis reaction of Ras, *Nat. Struct. Biol. 4*, 686−689.
36. Shurki, A., and Warshel, A. (2004) Why does the Ras switch "break" by oncogenic mutations? *Proteins 55*, 1−10.
37. Warshel, A. (1991) *Computer Modeling of Chemical Reactions in Enzymes and Solutions*, John Wiley & Sons, New York.
38. Åqvist, J., and Warshel, A. (1993) Simulation of enzyme reactions using valence bond force fields and other hybrid quantum/classical approaches, *Chem. Rev. 93*, 2523−2544.
39. Shurki, A., and Warshel, A. (2003) Structure/function correlations of protreins using MM, QM/MM and related approaches; methods, concepts, pitfalls and current progress, *Adv. Protein Chem. 66*, 249−312.
40. Klahn, M., Rosta, E., and Warshel, A. (2006) On the mechanism of hydrolysis of phosphate monoesters dianions in solutions and proteins, *J. Am. Chem. Soc. 128*, 15310−15323.
41. Zwanzig, R. W. (1954) High-temperature equation of state by a perturbation method. I. Nonpolar gases, *J. Chem. Phys. 22*, 1420.
42. Valleau, J. P., and Torrie, G. M. (1977) *Modern Theoretical Chemistry*, Vol. 5, Plenum Press, New York.
43. Hwang, J.-K., and Warshel, A. (1987) Microscopic examination of free energy relationships for electron transfer in polar solvents, *J. Am. Chem. Soc. 109*, 715−720.
44. Hwang, J.-K., King, G., Creighton, S., and Warshel, A. (1988) Simulation of free energy relationships and dynamics of S_N2 reactions in aqueous solution, *J. Am. Chem. Soc. 110*, 5297−5311.
45. King, G., and Warshel, A. (1990) Investigation of the free energy functions for electron transfer reactions, *J. Chem. Phys. 93*, 8682−8692.
46. Lee, F. S., Chu, Z. T., and Warshel, A. (1993) Microscopic and semimicroscopic calculations of electrostatic energies in proteins by the POLARIS and ENZYMIX programs, *J. Comput. Chem. 14*, 161−185.
47. Chu, Z. T., Villa, J., Štrajbl, M., Schutz, C. N., Shurki, A., and Warshel, A. (2004) in *Preparation*, University of Southern California, Los Angeles, CA.
48. King, G., and Warshel, A. (1989) A surface constrained all-atom solvent model for effective simulations of polar solutions, *J. Chem. Phys. 91*, 3647−3661.
49. Lee, F. S., and Warshel, A. (1992) A local reaction field method for fast evaluation of long-range electrostatic interactions in molecular simulations, *J. Chem. Phys. 97*, 3100−3107.
50. Lee, F. S., Chu, Z. T., Bolger, M. B., and Warshel, A. (1992) Calculations of antibody-antigen interactions: microscopic and semi-microscopic evaluation of the free energies of binding of phosphorylcholine analogs to McPC603, *Protein Eng. 5*, 215−228.
51. Kubo, R., Toda, M., and Hashitsume, N. (1985) *Statistical Physics II: Nonequilibrium Statistical Mechanics*, Springer-Verlag, Berlin, Germany.
52. Muegge, I., Schweins, T., Langen, R., and Warshel, A. (1996) Electrostatic control of GTP and GDP binding in the oncoprotein p21 ras, *Structure 4*, 475−489.
53. These results seem to differ from the results obtained by Klähn et al. (*40*). However, as can be concluded from their study, the reaction coordinate choice is crucial for a correct description of the reaction profile, and a proper reaction coordinate should account for all of the system's degrees of freedom. While Klähn et al. utilized only two bond distances to define the reaction coordinate, we defined our reaction coordinate as the difference between the corresponding VB states, which in turn ensures the inclusion of all of the system's degrees of freedom. In addition, while Klähn et al. calculated only the minimal energy path, using the FEP/US approach, we calculated the free energy surface. Therefore, differences in the overall reaction profile of the hydrolysis in protein are expected.
54. Sucato, C. A., Upton, T. G., Kashemirov, B. A., Batra, V. K., Martinek, V., Xiang, Y., Beard, W. A., Pedersen, L. C., Wilson, S. H., McKenna, C. E., Florian, J., Warshel, A., and Goodman, M. F. (2007) Modifying the beta, gamma leaving-group bridging oxygen alters nucleotide incorporation efficiency, fidelity, and the catalytic mechanism of DNA polymerase beta, *Biochemistry 46*, 461−471.
55. It is noted that recent studies found an $H_2PO_4^-$ intermediate (Pi) in the ras-rasGAP complex and suggested that the release of this phosphate (Pi) from the protein is rate limiting (*56*). Our studies (work in progress) suggest that the product of the reaction is indeed very stable in ras-rasGAP, implying that a barrier is required for the release of the phosphate and that both the release and the hydrolysis can be rate limiting. However, in Gs_α, the product stabilization we obtained is minor. Thus, this fact, supported by the experimental data (*57*), lead us to believe that here the hydrolysis reaction is a key player in the determination of the barrier height.
56. Kotting, C., Blessenohl, M., Suveyzdis, Y., Goody, R. S., Wittinghofer, A., and Gerwert, K. (2006) A phosphoryl transfer intermediate in the GTPase reaction of Ras in complex with its GTPase-activating protein, *Proc. Natl. Acad. Sci. U.S.A. 103*, 13911−13916.
57. Berghuis, A. M., Lee, E., Raw, A. S., Gilman, A. G., and Sprang, S. R. (1996) Structure of the GDP-Pi complex of Gly203→G(i alpha 1): a mimic of the ternary product complex of G alpha-catalyzed GTP hydrolysis, *Structure 4*, 1277−1290.

58. Kotting, C., and Gerwert, K. (2004) Time-resolved FTIR studies provide activation free energy, activation enthalpy and activation entropy for GTPase reactions, *Chem. Phys. 307*, 227−232.
59. Kleuss, C., Raw, A. S., Lee, E., Sprang, S. R., and Gilman, A. G. (1994) Mechanism of GTP hydrolysis by G-protein alpha-subunits, *Proc. Natl. Acad. Sci. U.S.A. 91*, 9828−9831.
60. Schweins, T., Geyer, M., Scheffzek, K., Warshel, A., Kalbitzer, H. R., and Wittinghofer, A. (1995) Substrate-assisted catalysis as a mechanism for GTP hydrolysis of p21 ras and other GTP-binding proteins, *Nat. Struct. Biol. 2*, 36−44.
61. Shurki, A., Štrajbl, M., Schutz, C. N., and Warshel, A. (2004) Electrostatic basis for bioenergetics, *Methods Enzymol. 380*, 52−84.
62. Warshel, A., Sharma, P. K., Kato, M., Xiang, Y., Liu, H. B., and Olsson, M. H. M. (2006) Electrostatic basis for enzyme catalysis, *Chem. Rev. 106*, 3210−3235.
63. Brito, M., Guzman, L., Romo, X., Soto, X., Hinrichs, M. V., and Olate, J. (2002) (SN)-N-111 mutation in the helical domain of human Gs alpha reduces its GDP/GTP exchange rate, *J. Cell. Biochem. 85*, 615−620.
64. Hwang, J.-K., and Warshel, A. (1988) Why ion pair reversal by protein engineering is unlikely to succeed, *Nature 334*, 270.
65. Guangpu, L., and Xuejun, C. Z. (2004) GTP hydrolysis mechanism of Ras-like GTPases, *J. Mol. Biol. 340*, 921−932.
66. Wittinghofer, A. (2006) Phosphoryl transfer in Ras proteins, conclusive or elusive? *Trends Biochem. Sci. 31*, 20−23.
67. Glennon, T. M., Villa, J., and Warshel, A. (2000) How does GAP catalyze the GTPase reaction of Ras? A computer simulation study, *Biochemistry 39*, 9641−9651.

BI700585W